J Fluoresc (2014) 24:751–757
DOI 10.1007/s10895-014-1348-5

ORIGINAL PAPER

Morphological Effect on Fluorescence Behavior of Silver Nanoparticles

Mohammad Salman Khan · Vijay Raman Chaudhari

Received: 19 September 2013 / Accepted: 2 January 2014 / Published online: 15 January 2014

Abstract Effect of Silver nanoparticles (AgNPs) morphology on their fluorescence behavior is reported. AgNPs sol stabilized by Ethylene Diamine Tetra Acetic-Acid (EDTA) was prepared by chemical reduction method. Morphology of the AgNPs was tuned through changing the Ag^{+} ion concentration and P^{H} of reaction mixture. Additional peaks observed in surface Plasmon resonance spectra suggest the an-isotropic nature of AgNPs. Actual morphology was judged by Transmission Electron Microscopy. Emission spectra recorded using Spectrofluoremeter suggest the fluorescent nature of AgNPs, which also influenced by morphology of AgNPs and attributed to the variation in surface structure of an-isotropic AgNPs.

Keywords Silver nanoparticles · EDTA · Fluorescent behavior · Morphology effect · An-isotropy

Introduction

During last few decades, main focus of the nano-material research included development of novel synthetic strategies, tuning the morphologies, combination of different materials and understanding their physic-chemical properties [1–8]. Among various nano-materials, noble metals particularly silver and gold are most extensively studied due to their fascinating Surface Plasmon Resonance (SPR) properties, with major emphasis on the morphology dependent SPR behavior [9–11]. Impact of the SPR property is evolved in terms of technological development of sensors, detectors, DNA hybridization etc. [12–18]. Initial interest in Au NPs mainly arose from their high electron density that has been used for immune-staining with Au NPs as marker for transmission electron based imaging [19]. Later on, the plasmonic properties of Au NPs was widely used for colorimetric detection of biological molecules [20, 21]. Silver is another noble metal, which similar to gold, exhibits plasmonic properties in the nanometer scale and are the most studied system of colloidal metal NPs. Initially, AgNPs were considered because of their antibacterial activity [22–24]. Further interesting properties are observed for AgNPs that project them as potential material for diverse applications.

Recent emerging trend in this field is to synthesize the fluorescent metal nano-materials. Fedrigo et al. first time reported the fluorescence property of silver nano clusters (NCs) due to the discrete nature of band structure [25]. Huang and co-workers also demonstrated the fluorescence behavior of AgNCs due to the similar phenomenon [26]. In addition to the discreteness in band structure, fluorescence property can also be originate from the Ag(I) complex [27–30].

Recently, Pal et al. reported the fluorescence behavior of giant core shell particles, constituted of AgNCs shell on gold (I) surface [31], due to the synergistic effect of gold, silver and glutathione. Importance of the fluorescent metal nanoparticles relies on the Fluorescence-based detection technology, in combination with nanotechnology, and widely used in various fields [32–35]. A notable examples includes, application of fluorescent silver nanomaterial as colorimetric and PH sensor, detection of metal ions, indicators for biological detection, imaging guided therapy, surface PKa determination, temperature sensor, biological labeling [33, 36–47].

Efforts have also been made to increase fluorescence intensities of nanomaterial-based probes by fabricating metal −dye nano-composites [48], combination of metal NPs with

Electronic supplementary material The online version of this article (doi:10.1007/s10895-014-1348-5) contains supplementary material, which is available to authorized users.

M. S. Khan · V. R. Chaudhari (✉)
Department of Nano Science and Nano Technology, University Institute of Chemical Technology, North Maharashtra University, Umavi Nagar, Jalgaon 425 001, India
e-mail: vijay.rchaudhari@gmail.com

polymers and with other photo-active materials [49], where fluorescence intensity was found be enhanced by several folds in close proximity of metal NPs [50–52]. Further investigations on size dependent fluorescence behavior of AgNPs shows the red shift in fluorescence wavelength with the AgNCs size [53, 54]. However, gross understanding in this field requires the detail investigation for morphology effect on the fluorescence behavior of the AgNPs. As per our knowledge, there is hardly any reports that accounted the said point. Here we report the synthesis of fluorescent AgNPs by chemical route. Morphology of NPs was tuned by Ag^+ ion concentration and P^H of the reaction mixture. Noticeable morphological effect is observed on the fluorescence nature of the AgNPs.

Experimental Section

Chemicals & Materials

Silver nitrate (s.d.fine chemical Ltd.) and di-sodium salt of ethylene di-amine tetra-acetic acid (EDTA) (99.5 %, s.d.fine chemical Ltd.) Sodium hydroxide (97 %, Rankem Laboratory Reagent) L-Ascorbic acid (99.6 %, Himedia PCT0207-100 g) were used without further purifications. All the solutions were prepared using double distilled water.

Synthesis of AgNPs

Silver NPs were synthesized by chemical reduction method. Briefly, 25 mL $AgNO_3$ and 50 ml EDTA (12 mM) were taken in round bottom flask and stirred for 30 min. P^H of the solution was adjusted with 1 M NaOH solution and stirred for additional 15 min. Subsequently, 25 mL of ascorbic acid (2.5 mM) was added drop-wise. Nitrogen gas was bubbled throughout the reaction. Color of the solution turned colorless to color within couple of minutes after addition of ascorbic acid. The reaction mixture was allowed to stir for 30 min and finally diluted five times with double distilled water. Morphology of the NPs was controlled by varying the Ag^+ concentration and P^H of the reaction mixture. Details are tabulated in Table 1.

Characterization

The UV-visible spectra were recorded on a Shimadzu UV-1601 spectrophotometer. Emission spectra were recorded on a Shimadzu RF-5301 PC spectrofluore-meter. The morphology of nanoparticles was judged by Philips CM-200 super twin stem Transmission Electron Microscope (TEM) operated at 200 kV. Surface chemistry of AgNPs was analyzed by Fourier Transform Infrared Spectrophotometer Shimadzu FTIR-8400 range 400 cm^{-1} to 4,000 cm^{-1} resolution 4.0. X-ray diffraction (XRD) data were collected from deposited samples using a PAN alyticalX'pertpro MPD diffractometer with monochromatic Cu Kα radiation (λ=1.54056 Å)

Table 1 Details of the sample coding of AgNPs prepared under different experimental conditions

Sr. No.	Sample code	$[Ag^+]$ (25 mL)	pH
1	AgNP-1	2.5 mM	9.10
2	AgNP-2	2.5 mM	9.90
3	AgNP-3	1.0 mM	10.06
4	AgNP-4	5.0 mM	10.07
5	AgNP-5	2.5 mM	10.76
6	AgNP-6	5.0 mM	6.00

Results and Discussions

After addition of ascorbic acid, color of the reaction mixture slowly changes from colorless to orange color. Figure 1 depicts the UV-visible spectrum recorded on as prepared sol. A peak at 425 nm observed in the spectrum is assigned to the surface plasmon resonance (SPR) band for nano size silver, which arises due to collective oscillation of free electrons with respective to the positive core [55]. It suggest the formation of AgNPs in the solution.

To confirm the crystallographic phase, the X-ray diffractogram (XRD) was recorded on the dried sample and shown in Fig. 2. The major peaks at 38.4°, 44.4°, 64.6° and 77.57° due to [111], [200], [220] and [311] planes, respectively, fitted faithfully with the one reported for the cubic phase of silver [56]. Hence, based on SPR nature and XRD, formation of silver nanoparticles is concluded.

Surface composition of AgNPs was judged by recording FTIR spectrum and depicted in Fig. 3. For comparison, spectrum recorded using pure EDTA salt is also shown in the Figure. The prominent band observed at 3,600 cm^{-1} due to the O-H stretching in pure EDTA salt is stoke shifted at 3,432 cm^{-1} for AgNPs, which suggest the association of EDTA with Ag through O-H group. Moreover, the band at 3,080 cm^{-1} for C-H stretching of neat EDTA is disappeared for AgNPs advocate the further association of EDTA with Ag [57]. Therefore, FTIR spectra reveals the stabilization of AgNPs by EDTA, through [COO—Ag] and [C–Ag] complex formation.

A typical low-resolution TEM image obtained by drop-casting the sol onto TEM grid is shown in Fig. 4. An-isotropic morphology, close to hexagonal shape, is observed with average size ca. ~23 nm. Few bigger particles *ca.* 40 nm in size are also present. As prepared AgNPs sol was stable for the months. Zeta potential measurement indicated the −56 mV charge on the particle, which may provide them long term stability through electrostatic repulsion.

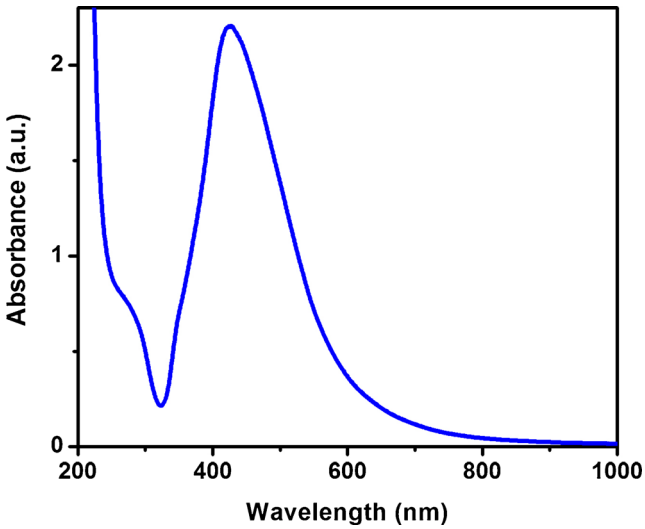

Fig. 1 UV-visible spectra recorded on the as prepared AgNPs sol

AgNPs sol showed fluorescent nature on illumination by UV light (Inset of Fig. 5). Therefore, fluorescent property was checked by recording emission spectra of AgNPs sol, as depicted in Fig. 5. Emission in blue-green region with broad peak centered at 470 nm is observed. Fluorescence is well above the signal-to-noise ratio and clearly visible by necked eyes. To confirmed the fluorescence nature of AgNPs, sol were subjected for dialysis (Sigma-Aldrich: Cellulose Membrane, MW=12 K_D, 9652-100 FT). Emission spectra recorded before and after dialysis are depicted in Fig. S1. Almost similar nature of emission spectra observed for both the cases confirmed the fluorescence nature of AgNPs. Moreover, emission spectra are recorded at different excitation wavelength and depicted in Fig. S2. After excitations at different wavelengths, emission wavelength remained same that further supports the fluorescent nature of AgNPs. Fluorescence behavior is reported for gold and silver NPs with size smaller than 2 nm

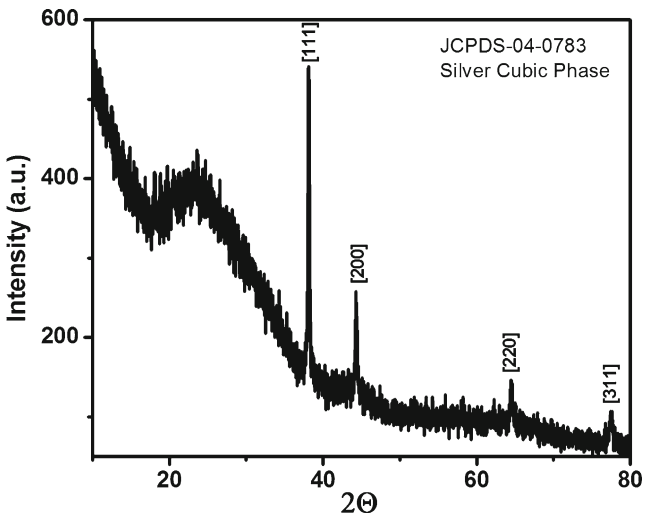

Fig. 2 X-ray diffractogram recorded on a vacuum-dried sample. The diffractogram is indexed by using JCPDS file 4-783

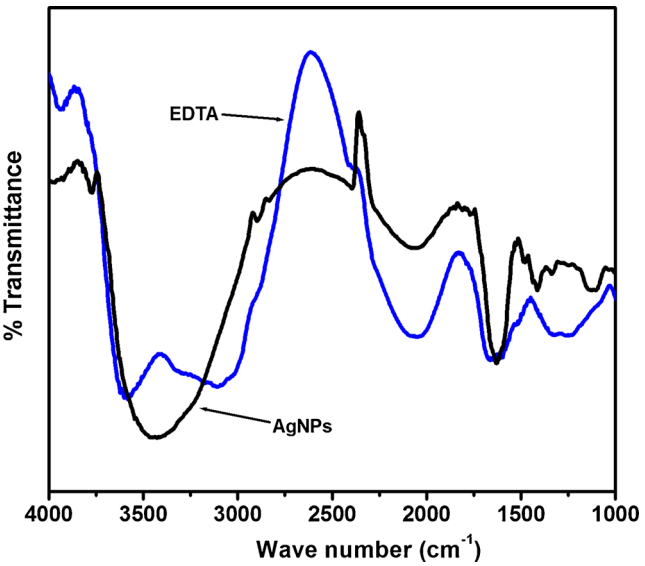

Fig. 3 FTIR spectra recorded on prestine EDTA salt and KBr pallet of AgNPs

and attributed to the origin of discreteness in band structure, i.e. Quantization Effect [26, 36, 47]. However, such quantization effect is ruled out in present case due to larger size of AgNPs. Recently, Pal et al. reported the fluorescent nature of Ag@Au giant particle where gold, silver and glutathione required in appropriate ratio to demonstrate the fluorescence behavior [31]. We also observed the photoluminescence property for AgNPs due to the DMSO complex formation on silver surface [5]. Similarly, other groups were also observed the fluorescence nature due to the Ag(I) complex. Therefore, observed fluorescence property for AgNPs can be attributed to the exciton generation from Ag-EDTA complex formation i.e. electron in the EDTA shell and the hole in the AgNPs.

The surface crystallographic structure of nano materials mainly depends on their shape [58, 59], and any variation in

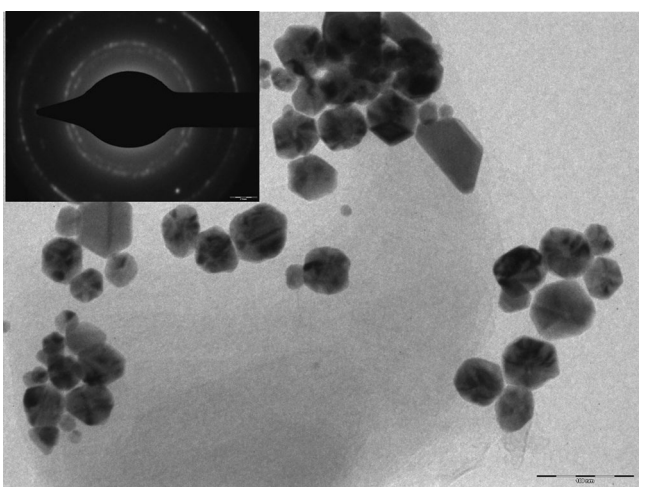

Fig. 4 Low-resolution TEM image recorded at 200 kV for the drop-casted AgNPs. Electron diffraction pattern is given in the inset. (Scale Bar is 100 nm)

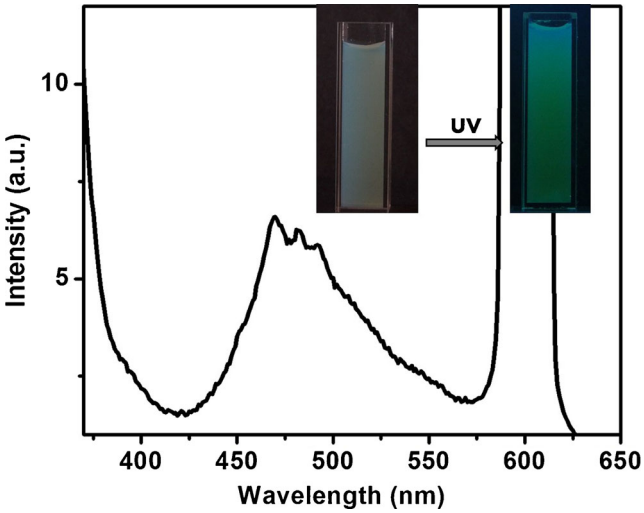

Fig. 5 Emission spectra recorded for AgNPs in aqueous medium. The excitation wavelength is 300 nm. *Inset* shows the photographic images recorded without and with UV light illumination of AgNPs sol

crystallographic structure due to the morphology can alters the energetics of Ag-EDTA complex. An investigation has been done by observing the fluorescence behavior for AgNPs having different morphology. Figure 6 depicts the TEM images recorded using AgNPs prepared by different experimental conditions. As can be seen, size increased from 8.5 to 56 nm for AgNP-1 to AgNP-6. Additionally, AgNPs undergoes shape evolutions. Briefly, roughly spherical shapes are presents for AgNP-1 with average size 8.5 nm. Major proportion of cubic shapes for AgNP-2 and roughly hexagon like structures for AgNP-6 are observed. An irregular shape is observed AgNP-3 and AgNP-5. Interestingly, TEM image for AgNP-4 shows interconnected chain like structure of NPs (Refer Inset). Therefore, one can summarize the results as, size of nanostructures increases from 8.5 to 56 nm and shape varies from roughly spherical to cubes, hexagonal, chain like interconnected structures and irregular shapes. EDTA has site selective binding ability which controls their growth mechanism [60]. Therefore, morphological evolution can be attributed to the post-growth effect of EDTA under different P^H conditions. It is further supported through the zeta potential measurements, where AgNPs possess zeta potential ranging from −20 to −80 mV for different morphology. Effect of morphology on

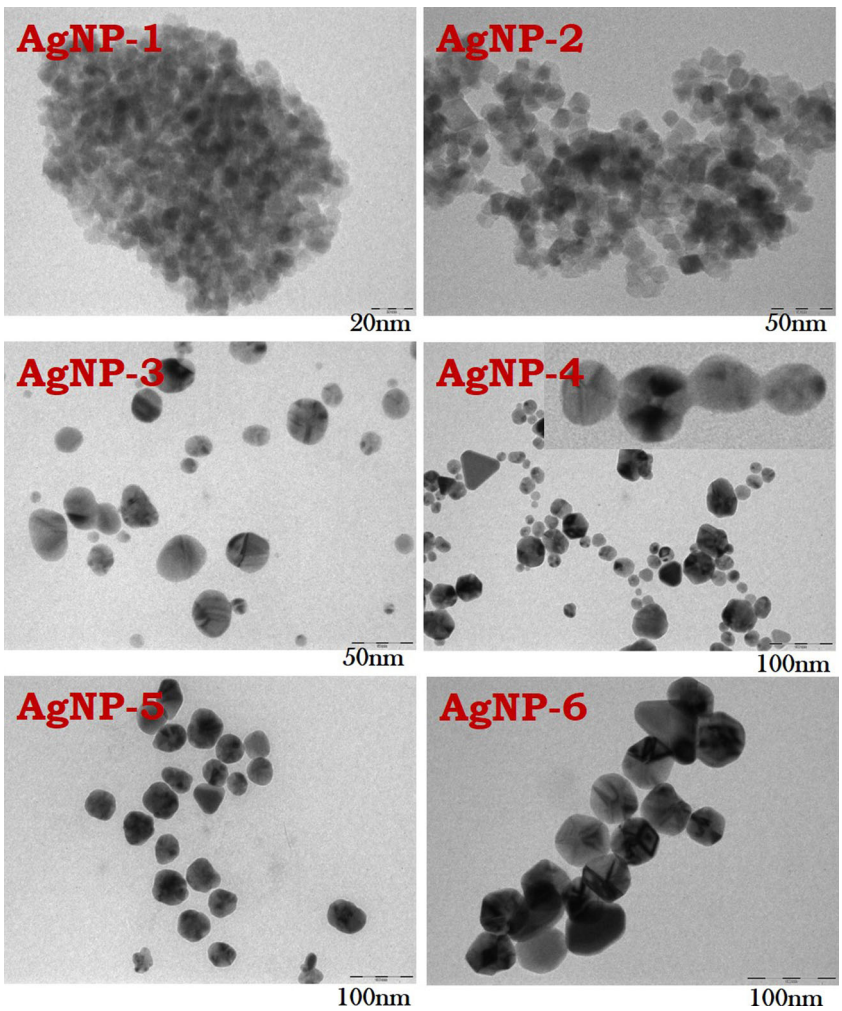

Fig. 6 TEM images recorded for AgNPs prepared under different experimental conditions. AgNPs are named as AgNPs-1, AgNPs-2, AgNPs-3, AgNPs-4, AgNPs-5 and AgNPs-6. Details of the experimental conditions are given in Table 1

its optical properties were studied by UV-visible and fluorescence spectroscopy. Figure 7 depicts the UV-visible spectra recorded using different morphology of AgNPs. Position and nature of SPR was found to be depend on morphology of nanostructures. In addition to main SPR peak, hump/telling is observed for the sample AgNP-2, AgNP-3 and AgNP-4. It is reported that, the quadrupole resonances are more active for anisotropic shaped particles and not for spheroidal one of roughly equivalent dimensions [55], which causes the multi-plasmon excitation, and results into multiple peaks. Further, DDA calculated spectra of cube exhibits multiple peaks due to the several distinct symmetries for dipole resonance compared with only one for the sphere [10, 61]. This is due to the segregation of charges at the corners which increased the charge separation, and thereby reduces the restoring force for electron oscillation [62], that in turn manifests itself in a red-shift of the resonance peak [10, 11, 63]. Therefore, an additional hump/tailing is attributed to the increase in axis length, sharpness of corners/edges in AgNPs shape [10, 64, 65]. It is supported by TEM images, where cubic, roughly hexagonal and interconnected NPs (similar to rod) are observed.

Figure 8a depicts the emission spectra recorded using AgNPs having different morphology. Roughly spherical nanostructures (AgNP-1, AgNP-5, AgNP-6) shows green fluorescence with peak centered at 468 nm. However, for an-isotropic nanostructures (AgNP-2, AgNP-3, AgNP-4) emission wavelength shifted from green to blue-green region with peak centered at 430 nm. In case of AgNPs-4, diffused nature of emission spectrum with low intensity is observed. Photographic images recorded using UV light illuminated AgNPs sol (Fig. 8b) elucidates the fluorescence behavior. AgNPs-1, AgNPs-5 and AgNPs-6 shows green fluorescence, while AgNPs-2, AgNPs-3 and AgNPs-4 shows blue-green color fluorescence, which is due to the morphological

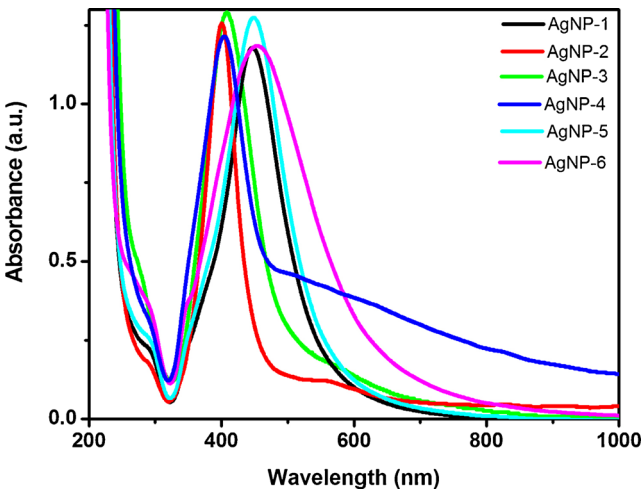

Fig. 7 UV-Visible spectra recorded for AgNPs prepared under different experimental conditions

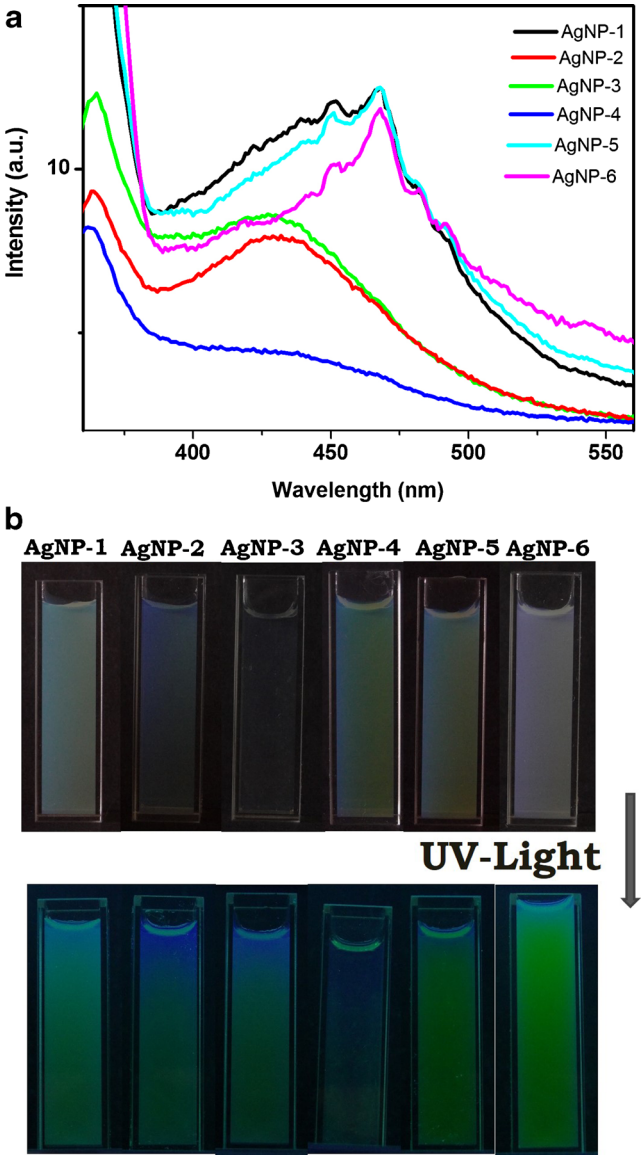

Fig. 8 **a** Emission spectra recorded for AgNPs prepared under different experimental conditions. Emission spectra are recorded using excitation wavelength at 300 nm. **b** Photographic images captured without and with UV light illumination of AgNPs sol

variation. Distinctly different nature of emission spectra of AgNP-4 can be attributed to the inter particle relaxation of exciton due to the close proximity of AgNPs. It is further supported by TEM images (Fig. 6, inset) where particles are attached to each other and forming chain like structures. An observed variation in fluorescence behavior is attributed to the morphological difference of AgNPs. Morphological variation in NPs alters their surface crystal structure and hence it's surface potential. Variation in surface potential affects an energetics of Ag-EDTA complex formed on surface of AgNPs and eventually an exciton energy, which may be responsible for the variation in fluorescence behavior. Time resolved fluorescence spectroscopy can provide the detail understanding, which will be the future plan of this work.

Conclusion

We have reported the synthesis of fluorescent AgNPs by chemical route. Fluorescent nature of AgNPs is attributed to the exciton generation due to electron from EDTA and hole from Ag core. Morphology of AgNPs were tuned by adjusting silver ion concentrations and P^H of the reaction mixture. Fluorescence property is found to be affected by morphology and attribute to the variation of surface crystal structure with morphology, that alters the Ag-EDTA complex energy and hence exciton energy.

Acknowledgments Authors thanks to University Grant Commission (UGC), New Delhi for financial support under Start-Up grant for newly recruited faculty. Authors also thanks to Indian Institute of Technology, Mumbai and Prof. J. V. Sali, School of Physical Sciences, North Maharashtra University, for TEM characterization and UV-Visible measurements, respectively.

References

1. Song Y, Garcia RM, Dorin RM, Wang H, Qiu Y, Coker EN, Steen WA, Miller JE, Shelnutt JA (2007) Synthesis of platinum nanowire networks using a soft template. Nano Lett 7:3650–3655
2. Sakamoto Y, Fukuoka A, Higuchi T, Shimomura N, Inagaki S, Ichikawa M (2004) Synthesis of platinum nanowires in organic–inorganic mesoporous silica templates by photoreduction: formation mechanism and isolation. J Phys Chem B 108:853–858
3. Piao Y, Lim H, Chang JY, Lee WY, Kim H (2005) Nanostructured materials prepared by use of ordered porous alumina membranes. Electrochim Acta 50:2997–3013
4. Chaudhari VR, Haram SK, Kulshreshtha SK, Bellare JR, Hassan PA (2007) Micelle assisted morphological evolution of silver nanoparticles. Colloids Surf A Physicochem Eng Asp 301:475–480
5. Wadkar MM, Chaudhari VR, Haram SK (2006) Synthesis and characterization of stable organosols of silver nanoparticles by electrochemical dissolution of silver in DMSO. J Phys Chem B 110:20889–20894
6. Samant KM, Chaudhari VR, Kapoor S, Haram SK (2007) Filling and coating of carbon nanotubes with silver by DC electrophoresis. Carbon 2126–2139
7. Zhao Q, Buongiorno NM, Lu W, Bernholc J (2005) Carbon nanotube −metal cluster composites: a new road to chemical sensors? Nano Lett 5:847–851
8. Melvina A, Vijay R, Chaudhari VR, Gupta B, Prakash R, Haram SK, Baskar G (2010) A facile methodology for the design of functionalized hollow silica spheres. J Colloid Interface Sci 346:265–269
9. Nikoobakht B, El-Sayed MA (2003) Preparation and growth mechanism of gold Nanorods (NRs) using seed-mediated growth method. Chem Mater 15:1957–1962
10. Wiley BJ, Im SH, Li ZY, McLellan J, Siekkinen A, Xia Y (2006) Maneuvering the Surface Plasmon Resonance of silver nanostructures through shape-controlled synthesis. J Phys Chem B 110:15666–15675
11. Mock JJ, Barbic M, Smith DR, Schultz DA, Schultz S (2002) Shape effects in plasmon resonance of individual colloidal silver nanoparticles. J Chem Phys 116:6755–6759
12. Kim EJ, Chung BH, Lee HJ (2012) Parts per trillion detection of Ni(II) ions by nanoparticle-enhanced Surface Plasmon Resonance. Anal Chem 84:10091–10096
13. Kwon MJ, Lee J, Wark AW, Lee HJ (2012) Nanoparticle-enhanced Surface Plasmon Resonance detection of proteins at attomolar concentrations: comparing different nanoparticle shapes and sizes. Anal Chem 84:1702–1707
14. Zynio SA, Samoylov AV, Surovtseva ER, Mirsky VM, Shirshov YM (2002) Bimetallic layers increase sensitivity of affinity sensors based on Surface Plasmon Resonance. Sensors 2:62–70
15. Li CZ, Male KB, Hrapovic S, Luong JHT (2005) Fluorescence properties of gold nanorods and their application for DNA biosensing. Chem Comm 3924–3926
16. Shipway AN, Katz E, Willner I (2000) Nanoparticle arrays on surfaces for electronic, optical, and sensor applications. Chem Phys Chem 1:18–52
17. Malinsky MD, Kelly KL, Schatz GC, Van Duyne RP (2001) Chain length dependence and sensing capabilities of the localized surface Plasmon resonance of silver nanoparticles chemically modified with alkanethiol self-assembled monolayers. J Am Chem Soc 123:1471–1482
18. Jung LS, Campbell CT, Chinowsky TM, Mar MN, Yee SS (1998) Quantitative interpretation of the response of Surface Plasmon Resonance sensors to adsorbed films. Langmuir 14:5636–5648
19. Sperling RA, Gil RP, Zhang F, Zanella M, Parak WJ (2008) Biological applications of gold nanoparticles. Chem Soc Rev 37:1896–1908
20. Leuvering JHW, Thal PJHM, Waart MVD, Schuurs AHWM (1980) Evaluation of a sol particle immunoassay for pregnancy detection. Fresenius J Anal Chem 301:132
21. Elghanian R, Storhoff JJ, Mucic RC, Letsinger RL, Mirkin CA (1997) Selective colorimetric detection of polynucleotides based on the distance-dependent optical properties of gold nanoparticles. Science 227:1078–1081
22. Morones J, Elechiguerra J, Camacho A, Holt K, Kouri J, Ram J, Yacaman M (2005) The bactericidal effect of silver nanoparticles. Nanotechnology 16:2346–2353
23. Baker C, Pradhan A, Pakstis L, Pochan DJ, Shah SI (2005) Synthesis and antibacterial properties of silver nanoparticles. J Nanosci Nanotechnol 5:244–249
24. Sondi I, Salopek-Sondi B (2004) Silver nanoparticles as antimicrobial agent: a case study on E. coli as a model for gram-negative bacteria. J Colloid Interface Sci 275:177–182
25. Fedrigo S, Harbich W, Buttet J (1993) Optical response of Ag_2, Ag_3, Au_2, and Au_3 in argon matrices. J Chem Phys 99:5712–5717
26. Huang S, Pfeiffer C, Hollmann J, Friede S, Chen JJC, Beyer A, Haas B, Volz K, Heimbrodt W, Martos JMM, Chang W, Parak WJ (2012) Synthesis and characterization of colloidal fluorescent silver nanoclusters. Langmuir 28:8915–8919
27. Yilmaz VT, Senel E, Guney E, Kazak C (2008) Two fluorescent silver(I)–saccharinato complexes of 2-methylpyrazine and pyrazine-2-carboxamide with Ag···Ag interactions. Inorg Chem Commun 11:1330–1333
28. Lobana TS, Khanna S, Butcher RJ (2008) Synthesis of a fluorescent gold(I) complex with a thiosemicarbazone, [Au2(3-NO2-Hbtsc)4]Cl2·2CH3CN. Inorg Chem Commun 11:1433–1435
29. Zhang S, Zhao Y (2011) Facile preparation of organic nanoparticles by interfacial cross-linking of reverse micelles and template synthesis of subnanometer Au−Pt nanoparticles. ACS Nano 5:2637–2646
30. Wu J, Fu Y, He Z, Han Y, Zheng L, Zhang J, Li W (2012) Growth mechanisms of fluorescent silver clusters regulated by polymorphic DNA templates: a DFT study. J Phys Chem B 116:1655–1665
31. Ganguly M, Pal A, Negishi Y, Pal T (2013) Synthesis of highly fluorescent silver clusters on Gold(I) surface. Langmuir 29:2033–2043
32. Rossi LM, Shi L, Quina FH, Rosenzweig Z (2005) Stöber synthesis of monodispersed luminescent silica nanoparticles for bioanalytical assays. Langmuir 21:4277–4280

33. Nakamura M, Masayuki S, Ishimura K (2007) Synthesis, characterization, and biological applications of multifluorescent silica nanoparticles. Anal Chem 79:6507–6514
34. Jain PK, Huang X, El-Sayed IH, El-Sayed MA (2007) Review of some interesting Surface Plasmon Resonance-enhanced properties of noble metal nanoparticles and their applications to biosystems. Plasmonics 2:107–118
35. Warner JH, Hoshino A, Yamamoto K, Tilley RD (2005) Water-soluble photoluminescent silicon quantum dots. Angew Chem Int Ed 44:4550–4554
36. Qu F, Li NB, Luo HQ (2013) Highly sensitive fluorescent and colorimetric pH sensor based on polyethylenimine-capped silver nanoclusters. Langmuir 29:1199–1205
37. Gianella A, Jarzyna PA, Mani V, Ramachandran S, Calcagno C, Tang J, Kann B, Dijk WJR, Thijssen VL, Griffioen AW, Storm G, Fayad ZA, Mulder WJM (2011) Multifunctional nanoemulsion platform for imaging guided therapy evaluated in experimental cancer. ACS Nano 5:4422–4433
38. Elavarasi M, Paul ML, Rajeshwari A, Chandrasekaran N, Mandal AB, Mukherjee A (2012) Studies on fluorescence determination of nanomolar Cr(III) in aqueous solutions using unmodified silver nanoparticles. Anal Methods 4:3407–3412
39. Childress ES, Roberts CA, Sherwood DY, LeGuyader CLM, Harbron EJ (2012) Ratiometric fluorescence detection of mercury ions in water by conjugated polymer nanoparticles. Anal Chem 84: 1235–1239
40. Chang CY, Chen CT, Li JL, Li JK, Wang HH, Kung FC, Shen JL, Chan WH, Yeh CK, Yeh HI, Lai WFT, Chang WH (2012) Rapid transformation of protein-caged nanomaterials into microbubbles as bimodal imaging agents. ACS Nano 6: 5111–5121
41. Maaden K, Sliedregt K, Kros A, Jiskoot W, Bouwstra J (2012) Fluorescent nanoparticle adhesion assay: a novel method for surface pKa determination of self-assembled monolayers on silicon surfaces. Langmuir 28:3403–3411
42. Ye F, Wu C, Jin Y, Chan YH, Zhang X, Chiu DT (2011) Ratiometric temperature sensing with semiconducting polymer dots. J Am Chem Soc 133:8146–8149
43. Lin CAJ, Yang TY, Lee CH, Huang SH, Sperling RA, Zanella M, Li JK, Shen JL, Wang HH, Yeh HI, Parak WJ, Chang WH (2009) Synthesis, characterization, and bioconjugation of fluorescent gold nanoclusters toward biological labeling applications. ACS Nano 3: 395–401
44. Disney MD, Zheng J, Seeberger PH (2004) Detection of bacteria with carbohydrate-functionalized fluorescent polymers. J Am Chem Soc 126:13343–13346
45. Nagao D, Yokoyama M, Yamauchi N, Matsumoto H, Kobayashi Y, Konno M (2008) Langmuir 24:9804–9808
46. Zhao X, Tapec-Dytioco R, Tan W (2003) Ultrasensitive DNA detection using highly fluorescent bioconjugated nanoparticles. J Am Chem Soc 125:11474–11475
47. Chen J, Jin Y, Fahruddin N, Zhao JX (2013) Development of gold nanoparticle-enhanced fluorescent nanocomposites. Langmuir 29: 1584–1591
48. Thomas KG, Kamat PV (2003) Chromophore-functionalized gold nanoparticles. Account Chem Res 36:888–898
49. Mahmoud MA, Poncheri AJ, El-Sayed MA (2012) Properties of π-conjugated fluorescence polymer–plasmonic nanoparticles hybrid materials. J Phys Chem C 116:13336–13342
50. Zhang J, Lakowicz JR (2007) Metal-enhanced fluorescence of an organic fluorophore using gold particles. Opt Express 15:2598–2606
51. Aslan K, Wu M, Lakowicz JR, Geddes CD (2007) Fluorescent core −shell Ag@SiO2 nanocomposites for metal-enhanced fluorescence and single nanoparticle sensing platforms. J Am Chem Soc 129: 1524–1525
52. Yang B, Lu N, Qi D, Ma R, Wu Q, Hao J, Liu X, Mu Y, Reboud V, Kehagias N, Torres CMS, Boey FYC, Chen X, Chi L (2010) Tuning the intensity of metal-enhanced fluorescence by engineering silver nanoparticle arrays. Small 6:1038–1043
53. Peyser LA, Vinson AE, Bartko AP, Dickson RM (2001) Photoactivated fluorescence from individual silver nanoclusters. Science 291:103–106
54. Badr Y, El A, Wahed MG, Mahmoud MA (2006) On 308 nm photofragmentation of the silver nanoparticles. Appl Surf Sci 253: 2502–2507
55. Kelly KL, Coronado E, Zhao LL, Schatz GC (2003) The optical properties of metal nanoparticles: the influence of size, shape, and dielectric environment. J Phys Chem B 107:668–677
56. JCPS – 04–0783
57. Kemp W (2009) Organic spectroscopy, 3rd edn. Palgrave
58. Li Y, Shi G (2005) Electrochemical growth of two-dimensional gold nanostructures on a thin polypyrrole film modified ITO electrode. J Phys Chem B 109:23787–23793
59. Li J, Wang LW (2003) Shape effects on electronic states of nanocrystals. Nano Lett 3:1357–1363
60. Belloni J, Mostafavi M, Remita H, Marignier JL, Delcourt MO (1998) Radiation-induced synthesis of mono- and multi-metallic clusters and nanocolloids. New J Chem 1239–1255.
61. Fuchs R (1975) Theory of the optical properties of ionic crystal cubes. Phys Rev B 11:1732–1740
62. Aizpurua J, Bryant GW, Richter LJ, Garca de Abajo FJ, Kelley BK, Mallouk T (2005) Optical properties of coupled metallic nanorods for field-enhanced spectroscopy. Phys Rev B 71:235420–13
63. Kottmann JP, Martin OJF, Smith DR, Schultz S (2001) Plasmon resonances of silver nanowires with a nonregular cross section. Phys Rev B 64:235402–10
64. Haes AJ, Haynes CL, McFarland AD, Schatz GC, Van Duyne RP, Zou S (2005) Plasmonic materials for surface-enhanced sensing and spectroscopy. MRS Bull 30:368–375
65. EL-Sayed MA (2001) Some interesting properties of metals confined in time and nanometer space of different shapes. Acc Chem Res 34: 257–264